Hindawi
Mathematical Problems in Engineering
Volume 2021, Article ID 9985870, 11 pages
https://doi.org/10.1155/2021/9985870

Research Article

New Tool Wear Estimation Method of the Milling Process Based on Multisensor Blind Source Separation

Chen Gao,[1] **Sun Bintao**,[2] **Heng Wu**,[3] **Mengjuan Peng**,[3] **and Yuqing Zhou**[2]

[1]*School of Mechatronics and Transportation, Jiaxing Nanyang Polytechnic Institute, Jiaxing, China*
[2]*College of Mechanical and Electrical Engineering, Wenzhou University, Wenzhou, China*
[3]*Wenzhou Hanggang Water Co. Ltd, Wenzhou, China*

Correspondence should be addressed to Sun Bintao; 381861064@qq.com

Received 5 March 2021; Revised 7 July 2021; Accepted 22 July 2021; Published 30 July 2021

Academic Editor: Akemi Gálvez

Timely and effective identification and monitoring of tool wear is important for the milling process. However, traditional methods of tool wear estimation have run into difficulties due to under small samples with less prior knowledge. This article addresses this issue by employing a multisensor tool wear estimation method based on blind source separation technology. Stationary subspace analysis (SSA) technology is applied to transform multisensor signals to stationary and nonstationary sources without prior information of signals. Ten dimensionless time-frequency indices of the nonstationary signal are extracted to train least squares support vector regression (LS-SVR) to obtain a tool wear estimation model for small samples. The analysis and comparison of one benchmark tool wear dataset and tool wear experiments verify the feasibility and effectiveness of the proposed method and outperform other two current methods.

1. Introduction

The computerized numerical control (CNC) milling machine provides an important source of power for hard machining. With the advantages of high automation and good precision, it is widely used in modern manufacturing. The cutter tool is the primary factor that affects the quality of the machine; its wear and damage can directly affect the surface quality of the workpiece as well as the machining efficiency. Tool wear accounts for 20–30% of the total downtime of a milling machine [1, 2], and tools and tool changes account for 3–12% of the total machining cost [3]. Therefore, online tool wear estimation has become an important research area in intelligent milling machining [4].

As shown in Figure 1, a typical online tool wear estimation method has three steps: (1) sensor signal acquisition, i.e., acquisition of physical field signals in the milling process by one or more sensors; (2) feature extraction, i.e., acquisition of received signals, such as by fast Fourier transform or wavelet analysis, to obtain information related to tool wear; and (3) monitoring, i.e., use of pattern recognition, neural networks, or regression analysis to classify or estimate tool failure.

In online tool wear estimation, many sensors have been used to obtain process signals [5], such as cutting force [6, 7], acoustic emission (AE) [8, 9], vibration [10, 11], and current [12, 13]. However, a single physical field signal has several shortcomings; for example, the cutting force is most sensitive to changes of tool wear, but commercial dynamometers are expensive and can increase manufacturing costs. An AE signal is measured at a high sampling rate, which leads to a large dataset and difficult processing and storage [14]. A vibration signal is difficult to filter, and it can be affected by the installation position. A current signal contains much noise, which makes it difficult to detect small fluctuations [15]. Due to the uncertainty and limitations of a single sensor, multisensor monitoring has become common due to its good performance and robustness [16]. Zhao et al. [17] applied a multisensor signal with a three-component dynamometer and three accelerometers to estimate tool wear using local feature-based gated recurrent unit networks. Zhou et al. [18] collected multisensor signals in a

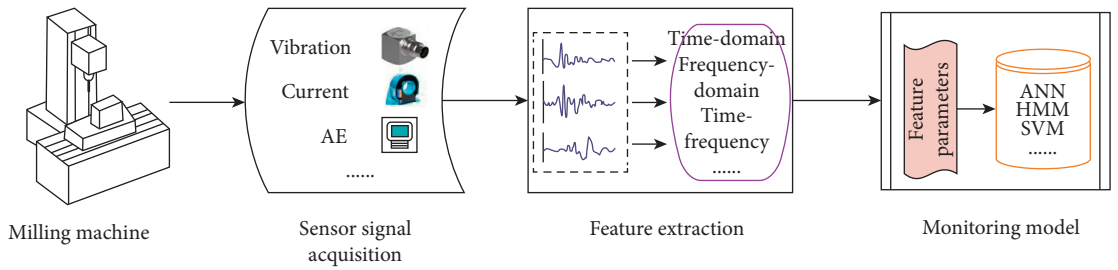

Figure 1: Process diagram of tool condition monitoring.

milling process and proposed a method to search for optimal feature parameter combinations in multisensor signals. Zhu et al. [19] proposed a smart tool condition monitoring system through several deep learning models with sensors, including cutting force, vibration, AE, CNC process data, and tool wear image. Multisensor methods can enhance the richness of information that contains potential tool wear levels and reduce the overall uncertainty of the measurement. In addition, several researchers determine the cutting tool life through mathematical methods. For example, Krolczyk et al. developed a mathematical model to predict the tool life by examining the influence of cutting parameters, namely, cutting speed, feed, and depth of cut onto tool life [20], researched the coated carbides tool life and the tool point surface topography [21], and analyzed the wear of milling cutters made of sintered carbide and of boron nitride [22], which provide a good theoretical basis for tool wear estimation. Moreover, hybrid intelligent methods have attracted considerable interest for tool fault diagnosis, e.g., wavelet transform (WT) and artificial neural network (ANN). The growth of deep learning (DL) in recent years has led to increasing interest in DL-based tool wear estimation methods [23, 24]. However, these hybrid intelligent methods require the signal analyzed to satisfy certain conditions, such as huge number of training samples, independent and identical distribution, white Gaussian noise, or prior information of data. For example, WT-based feature extraction lies in selecting a wavelet basis function that matches the fault characteristic waveform. However, it is difficult to select the appropriate wavelet basis function for the recognition of an unknown milling cutter tool fault [3]. DL-based methods require large amounts of training sample data, which are costly and time-consuming for machining processes [25]. Accordingly, these above conditions are difficult to meet in practical situation [26, 27], especially in time-varying and nonstationary nature of the NC machine complex cutting process. Moreover, there is little prior knowledge that can be available to detect and diagnose tool faults in NC machine currently [28]. The study of time-varying and nonstationary processes with less prior information is therefore well motivated. Therefore, obtaining good accuracy of tool wear estimation under small sample is currently a hot topic.

The main contributions of this article are as follows:

(1) A tool wear estimation method for a milling process based on a multisensor blind source separation method is proposed, using small training sample sizes and not presetting model parameters

(2) The proposed method based on SSA and LS-SVR significantly outperforms PCA according to milling tool wear experiments

(3) Experiments with different cutting conditions verify that the proposed method is robust and promising for milling tool condition monitoring

The remainder of this study is organized as follows. Section 2 describes the theoretical framework and proposed tool wear estimation method. Sections 3 and 4 verify the performance of the method with the benchmark PHM-2020 milling dataset and our tool wear experiments. Conclusions are given in Section 5.

2. Proposed Method

2.1. Framework. The proposed online milling tool wear estimation method includes the phases of model training and online tool wear estimation (Figure 2). During model training, multidimensional signals are collected for different tool wear and divided into several stationary sources and one nonstationary source by SSA technology (Section 2.2). Statistical parameters in the time and frequency domains (Section 2.3) of the nonstationary source are calculated to train the LS-SVR model (Section 2.4). In online tool wear estimation, for a new tool to be tested in milling operation, multidimensional signals are collected by multiple sensors and then extracted the nonstationary source by SSA. Statistical parameters in the time and frequency domains of the nonstationary source are calculated and input to the LS-SVR to estimate the wear value.

2.2. Stationary Subspace Analysis. SSA is a blind source separation algorithm proposed by von Bunau et al. [29]. In SSA, if two first-order parameters of a time series do not change with time, then it is stationary. SSA assumes that an observed multidimensional time series is a linear superposition of stationary sources that are constant over time and nonstationary sources that change with time [30]. An observed multidimensional time series $X \in \mathbf{R}^{D\times N}$ is defined as

$$X = AS_t = \begin{bmatrix} A^s & A^n \end{bmatrix} \begin{bmatrix} S_t^s \\ S_t^n \end{bmatrix}, \quad (1)$$

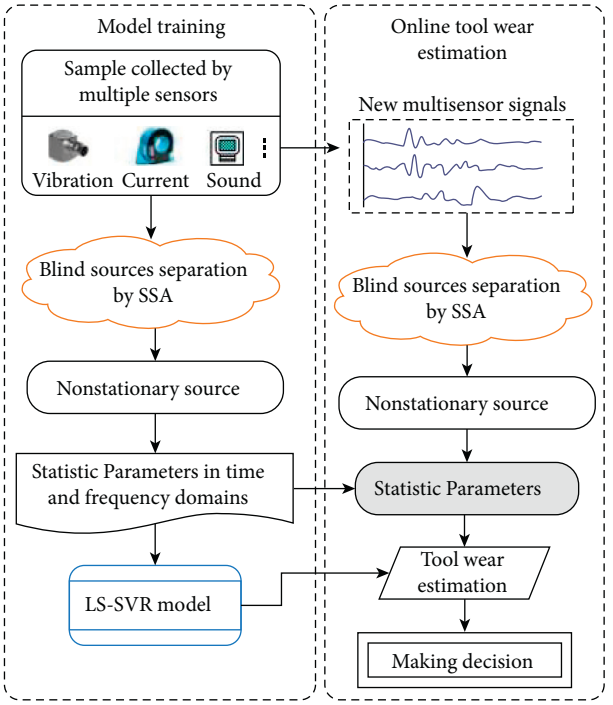

Figure 2: Framework of the proposed method.

where D and N are the dimension and number of data points, respectively; $A \in \mathbf{R}^{D\times D}$ is an unknown independent time matrix that is the linear superposition of the coefficient matrices of stationary and nonstationary sources; and S_t^s and S_t^n denote the d-dimensional stationary and $(D-d)$-dimensional nonstationary sources, respectively.

If d-dimensional stationary and $(D-d)$-dimensional nonstationary sources exist, then an inverse matrix A^{-1} can be constructed for the observation data X, such that

$$\begin{bmatrix} \widehat{S}_t^s \\ \widehat{S}_t^n \end{bmatrix} = A^{-1}X = A^{-1}A\begin{bmatrix} S_t^s \\ S_t^n \end{bmatrix} = \begin{bmatrix} B^sA^s & B^sA^n \\ B^nA^s & B^nA^n \end{bmatrix}\begin{bmatrix} S_t^s \\ S_t^n \end{bmatrix}. \quad (2)$$

To determine whether two first-order parameters of a time series change with time, the observed X is divided into continuous time segments, and each is compared with the whole time series through Kullback–Leibler (KL) divergence. The mean μ_i and covariance matrix Σ_i of each segment X_i are calculated, and KL divergence is employed to compare the changes of their mean and covariance, $X_i(\mu_i, \Sigma_i)$ and $X(\mu_0, \Sigma_0)$, respectively. The stationary index can be defined as

$$L(\mu_1, \ldots, \mu_n, \Sigma_1, \ldots, \Sigma_n) = \sum_{i=1}^{n} D_{KL}[N(\mu_i, \Sigma_i) \| N(\overline{\mu}, \overline{\Sigma})]. \quad (3)$$

To find the stationary mapping B, SSA minimizes the nonstationarity of the stationary direction to be estimated, and the optimal stationary mapping can be obtained by the solution of

$$\arg\min_{B\in R^{d\times d}} \sum D_{KL}\left[N\left(B_{\mu i}, B\Sigma_i B^T\right) \middle\| N\left(B_{\overline{\mu}}, B\overline{\Sigma}B^T\right)\right]. \quad (4)$$

To solve this problem, SSA uses an iterative operator to find B by updating an orthogonal matrix R. Starting from a random orthogonal matrix R_0, and in each step k, the steepest descent direction U in a set of orthogonal transformations is found using the standard gradient descent strategy, and the following update is performed until the last step $Q: R_{k+1} = UR_k$; then, we obtain $B^{s^*} = I_d R_Q W$, where W is the whitening matrix.

It can be seen that SSA does not need a large amount of sample data for training nor does it require independent dimension components. As long as the number of segmentation time is not less (generally greater than the dimension of the observed time series), the blind source analysis can be realized.

2.3. Statistical Parameters in Time and Frequency Domains. To overcome the drawback of features in a single domain, which lose some useful information related to the tool condition, we extract a few dimensionless statistical parameters in the time and frequency domains based on the literature [27, 31, 32] and our experimental studies [11, 33]. Table 1 lists 10 statistical feature parameters related to tool wear from the time and frequency domains that were extracted as feature parameters.

2.4. Least Squares Support Vector Regression. The aim of LS-SVR is to extract features from the original space and map the samples to a vector in a high-dimensional feature space, so as to solve the problem of linear indivisibility in the original space [34, 35].

Given a training set $D = \{(X_k, y_k) \mid k = 1, \ldots, M\}$, $X_k \in R^{D\times N}$, $y_k \in R$, X_k, and y_k denote independent and response variables, respectively. The response function to be estimated is

$$\begin{aligned} &\min_{\omega,b,c} J(\alpha, e) = \frac{1}{2}\alpha^T\alpha + c\sum_{k=1}^{N} e_k^2, \\ &\text{s.t. } y_k = \alpha^T\varphi(x_k) + b + e_k, \end{aligned} \quad (5)$$

where e_k is the error; α and b are the weight vector and bias, respectively, to be estimated; and $\varphi(\cdot)$ is a mapping function from low-dimensional space to high-dimensional feature space. The loss function J is the sum of squares due to error (SSE) and regularization of α. According to the Lagrange multiplier method, the following equation can be transformed [36]

$$L(\alpha, b, e; \gamma) = J(\alpha, e) - \sum_k \gamma_k\left\{\alpha^T\varphi(x_k) + b + e_k - y_k\right\}. \quad (6)$$

Let the partial derivatives of L to α, b, e, and γ be equal to 0. Eliminating e and γ, α and b to be estimated can be solved by the following matrix equation:

$$\begin{bmatrix} 0 & l_v^T \\ l_v & \Omega + \dfrac{I}{c} \end{bmatrix}\begin{bmatrix} b \\ \alpha \end{bmatrix} = \begin{bmatrix} 0 \\ y \end{bmatrix}, \quad (7)$$

Table 1: Ten statistical parameters.

Domain	Index	Formula
Time	Crest factor, T_{cf}	$T_{cf} = \max\{x_i\}/x_{rms}$
	Shape factor, T_{sf}	$T_{sf} = x_{rms}/(\sum \lvert x_i\rvert/n)$
	Kurtosis, T_{ku}	$T_{ku} = (\sum_{j=1}^{n} (x_j - T_{avg})^4)/(n \cdot T_{sd}^4) - 3$
	Skewness, T_{sk}	$T_{sk} = (\sum_{j=1}^{n} (x_j - T_{avg})^3)/(n \cdot T_{sd}^3)$
	Kurtosis factor, T_{kf}	$T_{kf} = T_{ku}/x_{rms}$
Frequency	Stabilization ratio, F_{sr}	$F_{sr} = (\sum_{j=1}^{n} f_j^2 P_i)/(\sqrt{\sum_{j=1}^{n} P}\sqrt{\sum_{j=1}^{n} f_j^4 P})$
	Wave-height ratio, F_{wr}	$F_{sr} = \max\{P_i\}/\sqrt{(2/n)\sum_{j=1}^{n/2} P_i^2}$
	Frequency high-low ratio, F_{fr}	$F_{fr} = \sum_{i=n/4}^{n/2} P_i / \sum_{i=1}^{n/4} P_i$
	Average frequency, F_{af}	$F_{af} = \sqrt{(\sum_{j=n/4}^{n/2} f_j P_j)/(\sum_{j=1}^{n/2} P_j)}$
	Modified equivalent bandwidth, F_{meb}	$F_{meb} = \sqrt{(\sum_{j=1}^{n} (f_j - \overline{f})^2 P_j)/(\sum_{j=1}^{n} P_j)}$

where $1_v = [1, \ldots, 1]$, and $\Omega_{kl} = \varphi(x_k)^T \varphi(x_l)$, $k, l = 1, \ldots, N$. LS-SVR employs a kernel function trick to overcome complex high-dimensional mapping operations of $\varphi(\cdot)$, such as a polynomial kernel, multilayer perceptual kernel, B-spline kernel, or RBF kernel.

$$\Psi(x_k, x_l) = \varphi(x_k)^T \varphi(x_l). \tag{8}$$

Thus, the response variable corresponding to a new observed X' can be determined as follows:

$$y(X') = \sum \alpha_k^* \Psi(X', X_k) + b^*. \tag{9}$$

In this study, the RBF kernel function is used, as given in the following equation, and the hyperparameter h is optimized by leave-one-out cross-validation (LOOCV) due to a small training sample set [37].

$$\psi_h(x, x') = \frac{1}{\sqrt{2\pi}} \exp\left(-\frac{(x - x')^2}{2h^2}\right). \tag{10}$$

3. Benchmark Dataset Analysis

3.1. Description of Dataset. The PHM-2010 challenge milling dataset employed for validation testing of the proposed method was obtained from a milling machine under dry milling using a 2-flute ball nose cutter [38, 39]. Figure 3 shows the device and sensors used in this experiment, and Table 2 lists the cutting parameters. There were three types of signals: cutting force from a three-component dynamometer, vibration from three accelerometers, and AE from an AE sensor. Therefore, each sample in the dataset included seven sensor channels' time series. The tool's flank wears were measured offline using a microscope after finishing each surface.

3.2. Analysis and Results. According to the data file, three cutter records, C1, C4, and C6, could be used to verify the performance of tool wear estimation. C4 and C6 were used as the training set, and C1 as the testing set.

For each sample, a seven-dimensional signal was obtained from six stationary and one nonstationary source, and the 10 dimensionless statistical parameters listed in Table 1 were calculated as the input of the LS-SVR. There are two reasons for selecting one nonstationary source: (1) it contains a variety of feature information than the stationary source to distinguish different tool wear; and (2) in the proposed method, it is easy to calculate the statistical parameters for the single nonstationary source.

To test the effectiveness of different methods, LS-SVR and principal component analysis (PCA) + LS-SVR were compared with the proposed SSA + LS-SVR. Ten

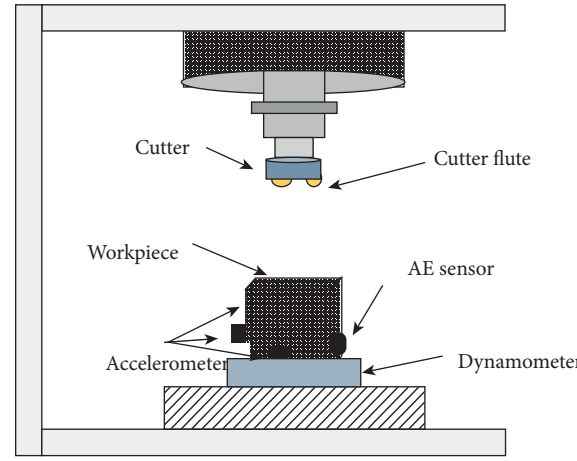

Figure 3: Experimental setup in the PHM-2010 challenge milling dataset.

Table 2: Operation parameters in the PHM-2010 challenge milling dataset.

Operation parameter	Value
CNC machine	Roders Tech RFM 760
Workpiece material	Inconel 718 (Jet engines)
Cutter	3-flute ball nose
Spindle speed	10400 rpm
Feed rate	1555 mm/min
Y depth of cut (radial)	0.125 mm
Z depth of cut (axial)	0.2 mm
Number of sensors	5
Number of sensor channels	7
Sampling data	50 kHz

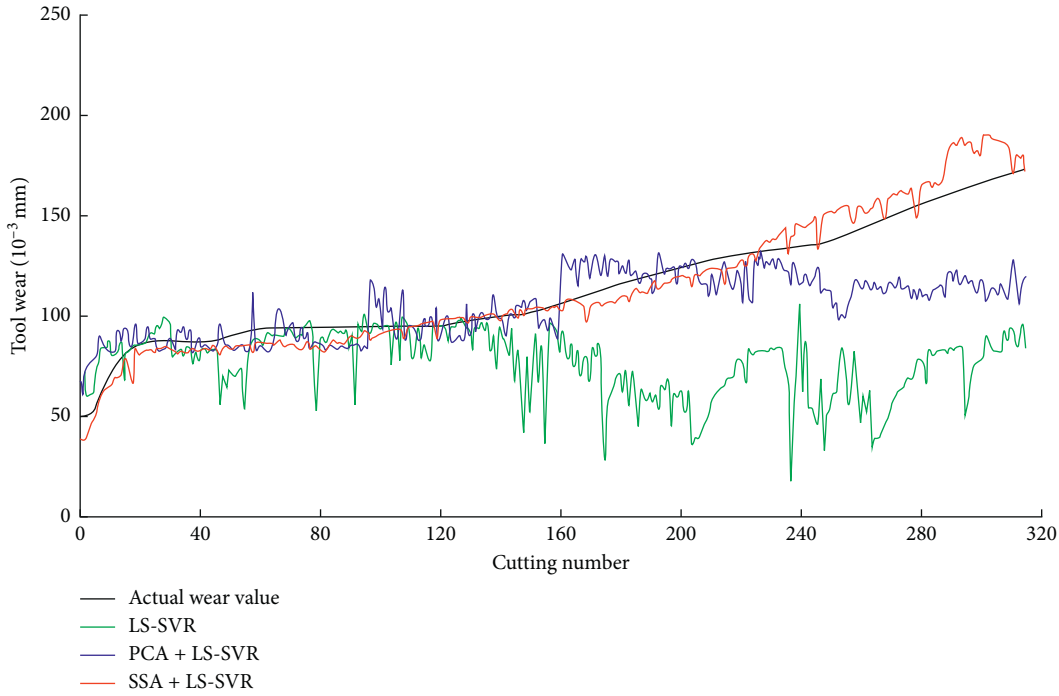

Figure 4: Comparison of three methods of tool wear estimation with testing set C1.

Table 3: Estimation error of three methods with testing set C1.

	LS-SVM	PCA + LS-SVM	SSA + LS-SVM
RMSE	52.1077	22.5284	8.4653
R	0.2899	0.6961	0.9848

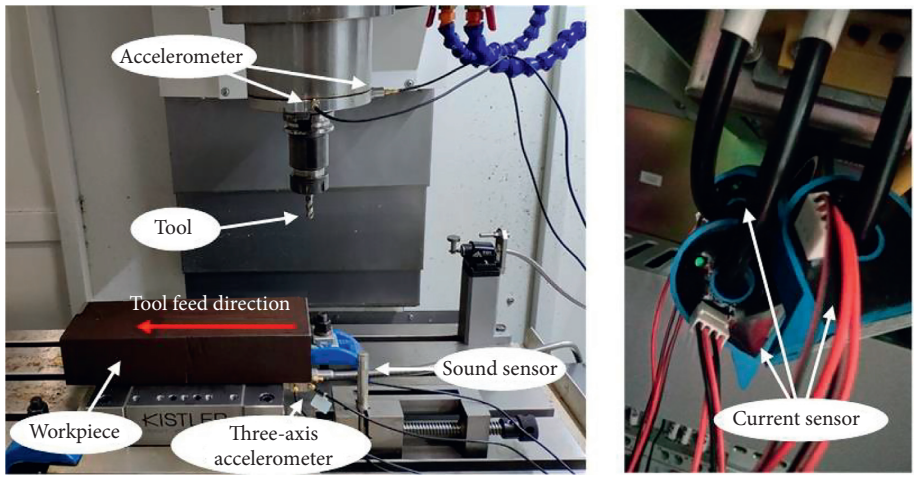

Figure 5: Experimental setup.

dimensionless statistical parameters of each dimension from the original multisensor signals were calculated directly for every sample and used as the input of the LS-SVR; there was no transformation of the original signal. PCA + LS-SVR uses PCA instead of SSA for feature extraction. Ten dimensionless statistical parameters of seven channels in each sample were calculated as the input of the PCA, and 10 principal components obtained by PCA were selected as the input of the LS-SVR. Root mean square error (RMSE) and the correlation coefficient (R) were employed to quantify the estimation performance of these methods.

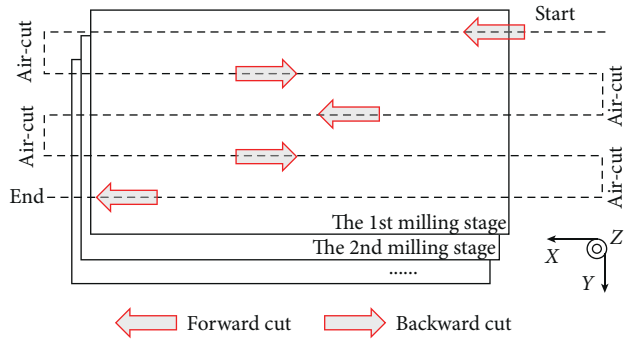

Figure 6: Milling path in the experiments.

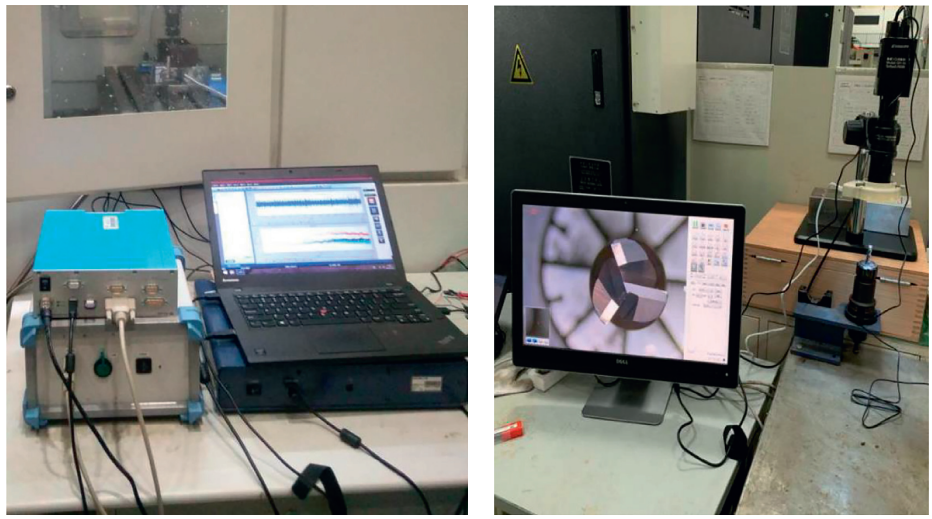

(a) (b)

Figure 7: Experimental measuring devices. (a) Data acquisition instrument. (b) Tool microscope.

Table 4: Cutting parameters in the experiment.

Tool	Spindle speed (rpm)	Depth of cut (mm)	Feed rate (mm/tooth)
1	2300	0.4	0.058
2	2300	0.4	0.072
3	2300	0.5	0.065
4	2300	0.6	0.072
5	2300	0.6	0.058
6	2400	0.4	0.065
7	2400	0.5	0.072
8	2400	0.6	0.058
9	2500	0.4	0.072
10	2500	0.4	0.058
11	2500	0.5	0.058
12	2500	0.6	0.065
13	2500	0.6	0.072
14	2500	0.6	0.058

The tool wear estimation results of tool C1 with three methods are shown in Figure 4, from which it can be seen that the estimation accuracy of the proposed method exceeds that of the other two methods. The error between the estimated and actual values of tool wear is presented in Table 3. The RMSE of the proposed SSA + LS-SVR method was

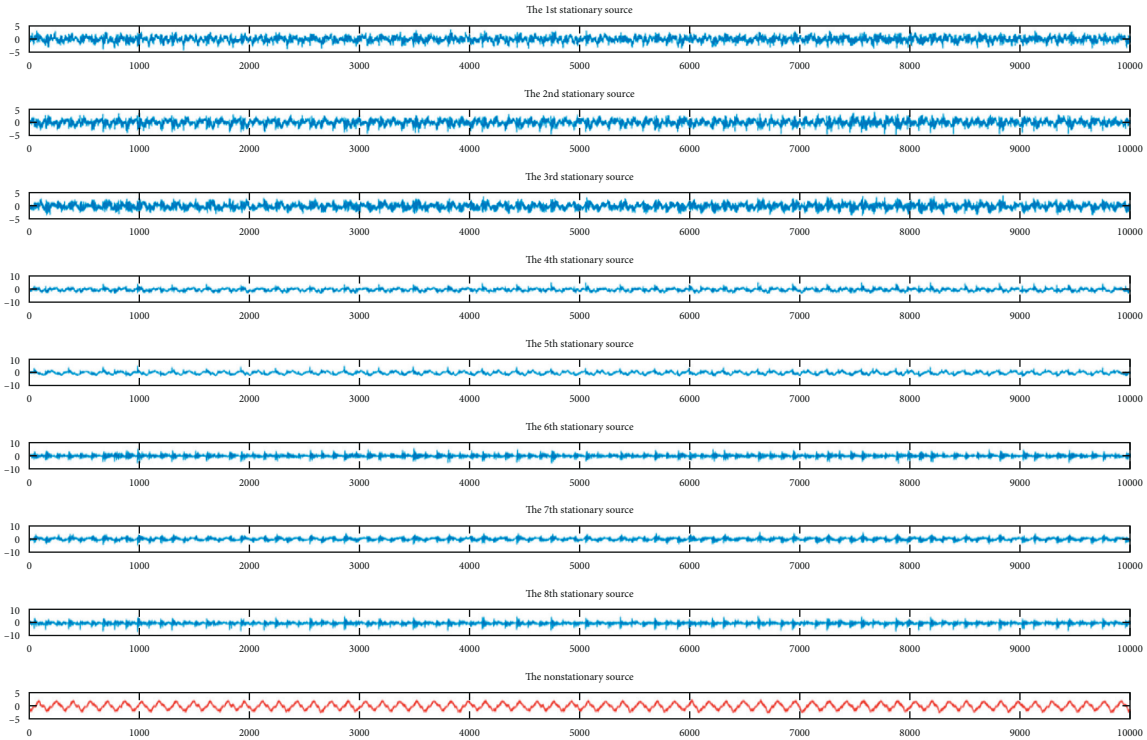

Figure 8: Signal after SSA transformation (tool wear value is 0.403 mm).

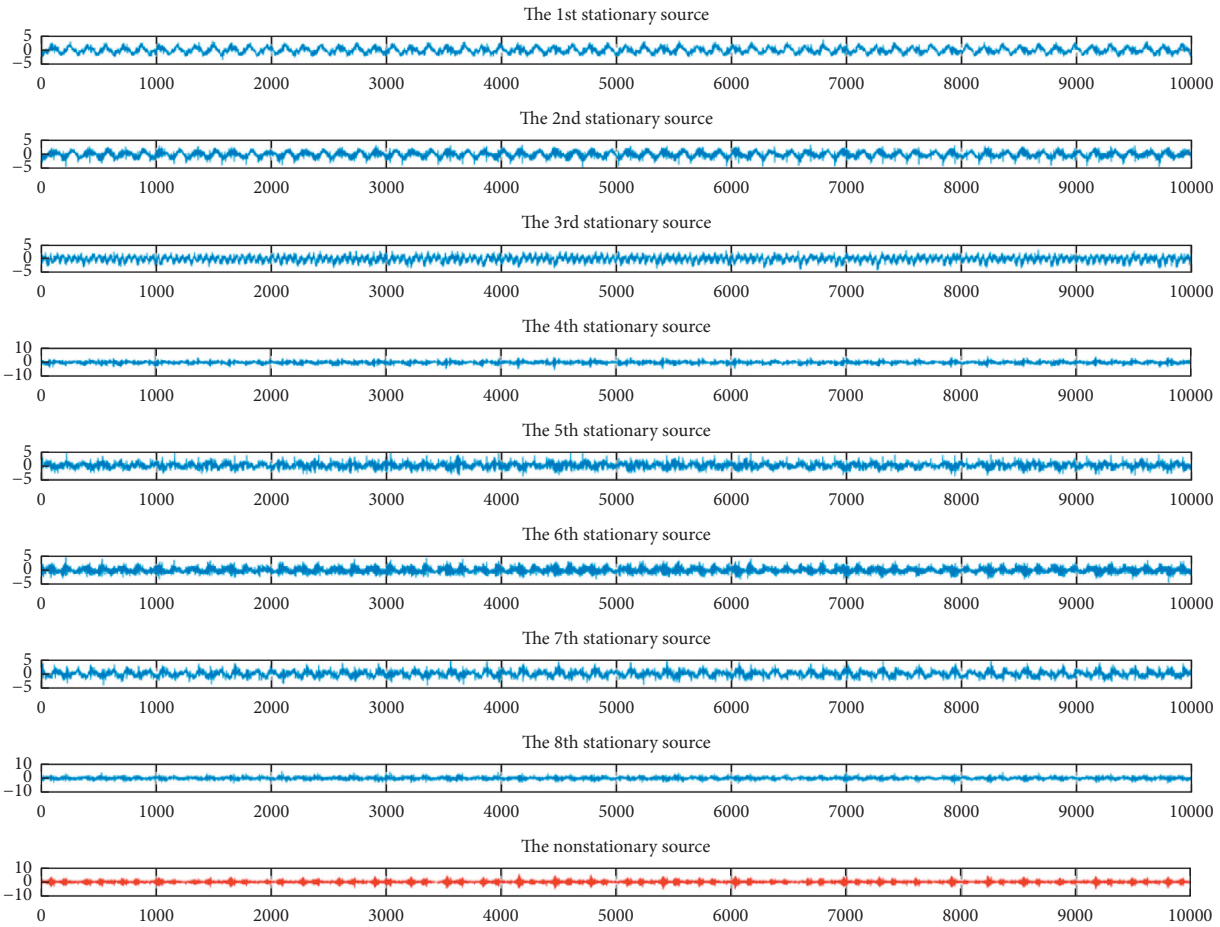

Figure 9: Signal after SSA transformation (tool wear value is 1.047 mm).

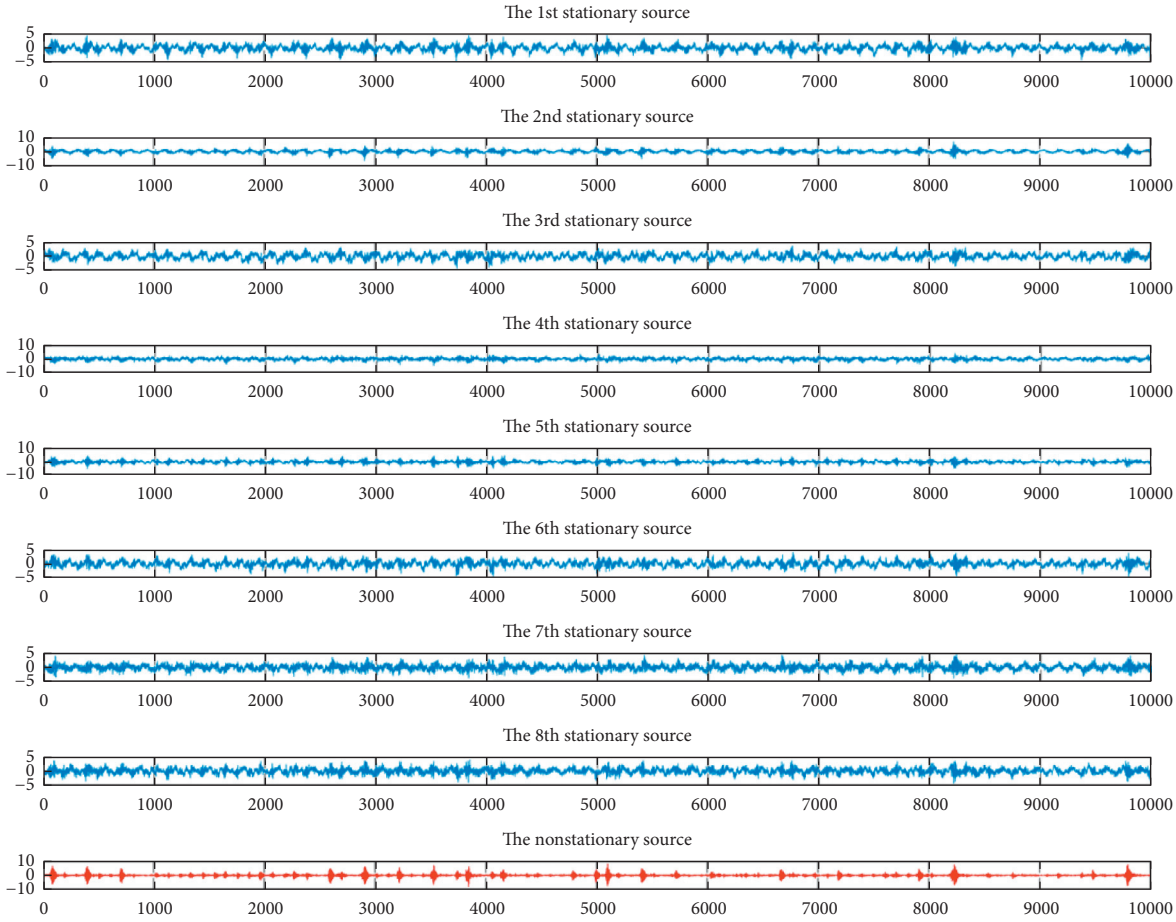

Figure 10: Signal after SSA transformation (tool wear value is 2.05 mm).

8.4653, which was 83.7% and 62.4% less than that of the LS-SVR and PCA + LS-SVR, respectively. R was 0.9848 for the proposed method, which was 0.69 and 0.28 greater than that of the LS-SVR and PCA + LS-SVR, respectively.

4. Experimental Investigation

4.1. Experimental Setup. Figure 5 shows the experimental setup for milling tool wear estimation under various operating conditions. The workpiece was #45 steel with dimensions of 300 mm × 100 mm × 80 mm, machined by a vertical machining center using an uncoated three-tooth tungsten steel end milling cutter under dry millings. Each cutting was completed five times in finishing a surface, i.e., three times forward and two times back, as shown in Figure 6. A three-axis accelerometer was mounted under the workpiece with a magnetic base to measure its vibrations in the X, Y, and Z directions, and accelerometers were attached to the side of the spindle by strong glue to measure the vibrations of the spindle in the X and Y directions. Three current sensors were clamped on the machine motor wires to measure the three-phase current of the motor. A sound sensor was fixed near the workpiece to measure sound during the cutting process. Therefore, the sensory data consisted of nine channels. These signals were collected by a data acquisition instrument and stored on a personal computer (Figure 7(a)), with a continuous sampling frequency of 12 kHz during the tool wear test. The wear value of each individual flute was measured offline using a tool microscope after machining a surface (Figure 7(b)).

There were 14 cutting tools used in our experiment with different cutting parameters, as given in Table 4. In each tool cutting experiment, there were five group signals after cutting a surface. The first four group signals were taken as training samples and the last as the test sample.

4.2. Analysis and Results. A nine-dimensional sensing signal in each sample was transformed by SSA and converted to eight stationary sources and one nonstationary source. The reason is the same as discussed in Section 3. Figures 8–10 show the transformation results through the SSA of tool 1 for three wear values (corresponding to the first, fifth, and tenth cutting). It can be seen that the time sequence diagram of the nonstationary source changes significantly after SSA transformation, while the changes of eight stationary sources after SSA transformation are not obvious. Therefore, we only used the signal of the nonstationary source to estimate tool wear. Here, as in Section 3, the RBF kernel was selected as the kernel function of the LS-SVR, and the hyperparameter was optimized by LOOCV.

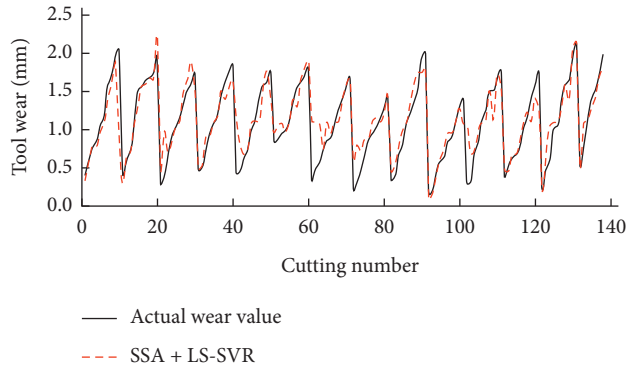

Figure 11: Tool wear estimation result with the proposed method.

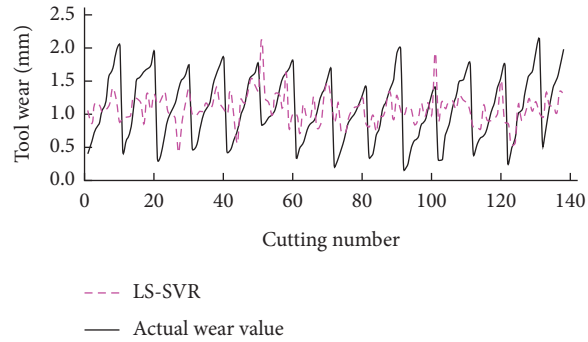

Figure 12: Tool wear estimation result with the LS-SVR method.

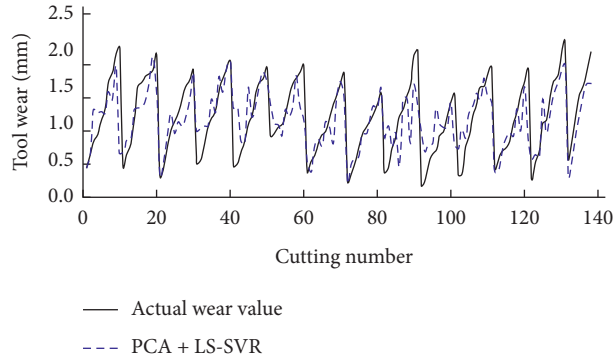

Figure 13: Tool wear estimation result with the PCA + LS-SVR method.

Table 5: Estimation error of three methods in the experiment.

	LS-SVM	PCA + LS-SVM	SSA + LS-SVM
RMSE	0.2309	0.1094	0.0529
R	0.3414	0.6701	0.8938

Figures 11–13 show the tool wear estimation results of the testing set with the three methods. The estimation error between the estimated and actual values of tool wear is given in Table 5. The RMSE of the proposed SSA + LS-SVR method was 0.0529, which is 77.1% and 51.6% less than that of the LS-SVR and PCA + LS-SVR, respectively. R of the proposed method was 0.8923, which is 0.55 and 0.22 higher than that of the LS-SVR and PCA + LS-SVR, respectively.

5. Conclusion

In order to solve the problem of low performance of traditional methods for milling tool wear estimation under small sample with less prior knowledge, a multisensor tool wear estimation method based on SSA and LS-SVR was proposed. Taking the advantage of SSA without prior information of signals and parameter presetting, the multidimensional signals collected by sensors were decomposed into stationary and nonstationary sources through SSA, and 10 dimensionless time-frequency statistical parameters from the nonstationary source were extracted as the input parameters of the LS-SVR to obtain the tool wear estimation model under small sample. The proposed SSA + LS-SVR method was validated on the PHM-2010 challenge milling benchmark dataset and our tool wear experiments. The results indicated that the root mean square error and correlation coefficient of the proposed method were significantly better than LS-SVR and PCA + LS-SVR on two milling TCM experiments. Furthermore, the proposed method could be improved to enhance its performance under one-dimensional signal for tool wear estimation, in which the number of subsources needs to be optimized.

Data Availability

The datasets used and analyzed to support the findings of this study are included within the article.

Conflicts of Interest

The authors declare that they have no conflicts of interest.

Acknowledgments

This work was supported in part by the Zhejiang Provincial Natural Science Foundation of China (LQ21E050003), in part by the National Natural Science Foundation of China (U1909217), and in part by the Fundamental Scientific Research Project of Wenzhou (G20190013).

References

[1] M. Malekian, S. S. Park, and M. B. G. Jun, "Tool wear monitoring of micro-milling operations," *Journal of Materials Processing Technology*, vol. 209, no. 10, pp. 4903–4914, 2009.

[2] J. Karandikar, T. Mcleay, S. Turner, and T. Schmitz, "Tool wear monitoring using naïve bayes classifiers," *International Journal of Advanced Manufacturing Technology*, vol. 77, no. 9-12, pp. 1613–1626, 2015.

[3] Y. Q. Zhou and W. Xue, "Review of tool condition monitoring methods in milling processes," *International Journal of Advanced Manufacturing Technology*, vol. 96, no. 5-8, pp. 2509–2523, 2018.

[4] Z. Huang, J. Zhu, J. Lei, X. Li, and F. Tian, "Tool wear predicting based on multi-domain feature fusion by deep convolutional neural network in milling operations," *Journal of Intelligent Manufacturing*, vol. 31, no. 4, pp. 953–966, 2020.

[5] Y. Zhou, B. Sun, W. Sun, and Z. Lei, "Tool wear condition monitoring based on a two-layer angle kernel extreme learning machine using sound sensor for milling process," *Journal of Intelligent Manufacturing*, vol. 9, 2020.

[6] H. Zhang, J. Zhao, F. Wang, J. Zhao, and A. Li, "Cutting forces and tool failure in high-speed milling of titanium alloy tc21 with coated carbide tools," *Proceedings of the Institution of Mechanical Engineers, Part B: Journal of Engineering Manufacture*, vol. 229, no. 1, pp. 20–27, 2015.

[7] Q. S. Zhu, B. T. Sun, Y. Q. Zhou, W. F. Sun, and J. W. Xiang, "Sample augmentation for intelligent milling tool wear condition monitoring using numerical simulation and generative adversarial network," *IEEE Transactions on Instrumentation and Measurement*, vol. 70, Article ID 3516610, 2021.

[8] G. Vetrichelvan, S. Sundaram, S. S. Kumaran, and P. Velmurugan, "An investigation of tool wear using acoustic emission and genetic algorithm," *Journal of Vibration and Control*, vol. 21, no. 15, pp. 3061–3066, 2014.

[9] M. T. Mathew, P. S. Pai, and L. A. Rocha, "An effective sensor for tool wear monitoring in face milling: acoustic emission," *Sadhana*, vol. 33, no. 3, pp. 227–233, 2008.

[10] P. Y. Sevilla-Camacho, J. B. Robles-Ocampo, and J. Muñiz-Soria, "Tool failure detection method for high-speed milling using vibration signal and reconfigurable bandpass digital filtering," *International Journal of Advanced Manufacturing Technology*, vol. 81, no. 5-8, pp. 1–8, 2015.

[11] Y. Q. Zhou, X. F. Liu, F. P. Li, B. T. Sun, and W. Xue, "An online damage identification approach for numerical control machine tools based on data fusion using vibration signals," *Journal of Vibration and Control*, vol. 21, no. 15, pp. 2925–2936, 2015.

[12] M. Ritou, S. Garnier, B. Furet, and J. Y. Hascoet, "Angular approach combined to mechanical model for tool breakage detection by eddy current sensors," *Mechanical Systems and Signal Processing*, vol. 44, no. 1-2, pp. 211–220, 2014.

[13] P. Stavropoulos, A. Papacharalampopoulos, E. Vasiliadis, and G. Chryssolouris, "Tool wear predictability estimation in milling based on multi-sensorial data," *International Journal of Advanced Manufacturing Technology*, vol. 82, no. 1–4, pp. 509–521, 2016.

[14] B. Cuka and D. W. Kim, "Fuzzy logic based tool condition monitoring for end-milling," *Robotics and Computer-Integrated Manufacturing*, vol. 47, 2017.

[15] R. Koike, K. Ohnishi, and T. Aoyama, "A sensorless approach for tool fracture detection in milling by integrating multi-axial servo information," *CIRP Annals*, vol. 65, no. 1, pp. 385–388, 2016.

[16] H. Liu, Z. Liu, W. Jia, X. Lin, and S. Zhang, "A novel transformer-based neural network model for tool wear estimation," *Measurement Science and Technology*, vol. 31, no. 6, Article ID 065106, 2020.

[17] R. Zhao, D. Wang, R. Yan, K. Mao, F. Shen, and J. Wang, "Machine health monitoring using local feature-based gated recurrent unit networks," *IEEE Transactions on Industrial Electronics*, vol. 65, no. 2, pp. 1539–1548, 2018.

[18] Y. Zhou, B. Sun, and W. Sun, "A tool condition monitoring method based on two-layer angle kernel extreme learning machine and binary differential evolution for milling," *Measurement*, vol. 166, Article ID 108186, 2020.

[19] K. Zhu, G. Li, and Y. Zhang, "Big data oriented smart tool condition monitoring system," *IEEE Transactions on Industrial Informatics*, vol. 16, no. 6, pp. 4007–4016, 2020.

[20] G. Krolczyk, M. Gajek, and S. Legutko, "Predicting the tool life in the dry machining of duplex stainless steel," *Eksploatacja I*

Niezawodnosc-Maintenance and Reliability, vol. 15, no. 1, pp. 62–65, 2013.

[21] G. M. Krolczyk, P. Nieslony, and S. Legutko, "Determination of tool life and research wear during duplex stainless steel turning," *Archives of Civil and Mechanical Engineering*, vol. 15, no. 2, pp. 347–354, 2015.

[22] P. Twardowski, S. Legutko, G. Krolczyk, and S. Hloch, "Investigation of wear and tool life of coated carbide and cubic boron nitride cutting tools in high speed milling," *Advances in Mechanical Engineering*, vol. 7, no. 6, pp. 1–9, 2015.

[23] X.-C. Cao, B.-Q. Chen, B. Yao, and W.-P. He, "Combining translation-invariant wavelet frames and convolutional neural network for intelligent tool wear state identification," *Computers in Industry*, vol. 106, pp. 71–84, 2019.

[24] G. Serin, B. Sener, A. M. Ozbayoglu, and H. O. Unver, "Review of tool condition monitoring in machining and opportunities for deep learning," *International Journal of Advanced Manufacturing Technology*, vol. 109, no. 3-4, pp. 953–974, 2020.

[25] G. Zhi, D. He, W. Sun, Y. Zhou, X. Pan, and C. Gao, "An edge-labeling graph neural network method for tool wear condition monitoring using wear image with small samples," *Measurement Science and Technology*, vol. 32, no. 6, Article ID 064006, 2021.

[26] A. J. Torabi, J. E. Meng, X. Li, and B. S. Lim, "A survey on artificial intelligence-based modeling techniques for high speed milling processes," *IEEE System Journal*, vol. 9, pp. 1069–1080, 2014.

[27] S. Manouchehr and T. TavakoliKian, "A review on the artificial neural network approach to analysis and prediction of seismic damage in infrastructure," *International Journal of Hydromechatronics*, vol. 2, no. 4, pp. 178–196, 2019.

[28] M. Lamraoui, M. Thomas, and M. El Badaoui, "Cyclostationarity approach for monitoring chatter and tool wear in high speed milling," *Mechanical Systems and Signal Processing*, vol. 44, no. 1-2, pp. 177–198, 2014.

[29] P. von Bünau, F. C. Meinecke, F. C. Király, and K.-R. Müller, "Finding stationary subspaces in multivariate time series," *Physical Review Letters*, vol. 103, no. 21, Article ID 214101, 2009.

[30] M. Kawanabe, W. Samek, P. von Bünau, and F. C. Meinecke, "An information geometrical view of stationary subspace analysis," in *Proceedings of Artificial Neural Networks and Machine Learning-ICANN 2011*, pp. 397–404, Espoo, Finland, June 2011.

[31] A. Kumar and R. Kumar, "Adaptive artificial intelligence for automatic identification of defect in the angular contact bearing," *Neural Computing and Applications*, vol. 29, no. 8, pp. 277–287, 2018.

[32] L. Cui, B. Li, J. Ma, and Z. Jin, "Quantitative trend fault diagnosis of a rolling bearing based on Sparsogram and Lempel-Ziv," *Measurement*, vol. 128, pp. 410–418, 2018.

[33] C. Gao, W. Xue, Y. Ren, and Y. Zhou, "Numerical control machine tool fault diagnosis using hybrid stationary subspace analysis and least squares support vector machine with a single sensor," *Applied Sciences*, vol. 7, no. 4, p. 346, 2017.

[34] K. Huang, M. Y. You, Y. X. Ye, B. Jiang, and A. N. Lu, "Direction of arrival based on the multioutput least squares support vector regression model," *Mathematical Problems in Engineering*, vol. 2010, Article ID 8601376, 8 pages, 2020.

[35] X. Liu, A. Ouyang, and Z. Yun, "Fuzzy weighted least squares support vector regression with data reduction for nonlinear system modeling," *Mathematical Problems in Engineering*, vol. 2018, Article ID 7387650, 13 pages, 2018.

[36] A. Kumar and R. Kumar, "Least square fitting for adaptive wavelet generation and automatic prediction of defect size in the bearing using levenberg-marquardt backpropagation," *Journal of Nondestructive Evaluation*, vol. 36, no. 1, p. 7, 2017.

[37] B. R. Murlidhar, R. K. Sinha, E. T. Mohamad, R. Sonkar, and M. Khorami, "The effects of particle swarm optimisation and genetic algorithm on ANN results in predicting pile bearing capacity," *International Journal of Hydromechatronics*, vol. 3, no. 1, pp. 69–87, 2020.

[38] The Prognostics and Health Management Society, "Conference data challenge," 2010, https://www.phmsociety.org/competition/phm/10.

[39] T. Benkedjouh, N. Zerhouni, and S. Rechak, "Tool wear condition monitoring based on continuous wavelet transform and blind source separation," *The International Journal of Advanced Manufacturing Technology*, vol. 97, no. 9–12, pp. 3311–3323, 2018.